Journal of Supramolecular Structure 2:538–557 (1974)

A MOLECULAR MODEL OF MEMBRANE EXCITABILITY

Gilbert Baumann and Paul Mueller

Department of Molecular Biology, Eastern Pennsylvania Psychiatric Institute, Philadelphia, Pennsylvania

Alamethicin, monazomycin, or EIM induce electrical excitability in lipid bilayers. The voltage-dependent gating displays all the characteristics observed in excitable cells and its basic features can be quantitatively described by the Hodgkin-Huxley equations.

A common molecular mechanism of membrane excitation has been postulated. It assumes that in the absence of an electrical field the channel-forming molecules lie at the surface of the membrane. An applied potential tilts them from the surface into the hydrocarbon region of the bilayer. Once in this position the molecules diffuse laterally and form aggregates which act as channels for the flow of ions.

In the case of alamethicin we assume that the molecule forms an elongated ellipsoid with two glutamic residues at one end, and a metal ion in four- or five-fold coordination with peptide carbonyl oxygens at the other. An applied field pulls the cationic end through the membrane to the other side, while the glutamic residues hold the other end attached to the original surface. The molecules now span the membrane and aggregate, forming oligomeric channels in which most of the peptide carbonyls face toward the center, and the methyl groups outward.

Monomers and dimers do not conduct and an individual channel can have different conductance values depending on the number of monomers in the aggregate and the resulting channel diameter. A quantitative description of this process matches observed gating kinetics, gating currents, and the single channel conductance increments. Without additional assumptions, inactivation follows directly from the aggregation process because with proper rate constants, the average degree of polymerization and therefore number of open channels goes through a maximum in time.

The model may also apply to the excitation process of higher cells.

INTRODUCTION

Alamethicin (1), monazomycin (2), and EIM (3) are compounds inducing electrical excitability and action potentials in lipid bilayer membranes (4, 5). Alamethicin is a cyclic peptide, EIM is a protein, and monazomycin seems related to the polyene anti-

biotics. In bilayers containing these compounds the steady-state and kinetic dependence of the membrane conductance on the potential is very much the same as that observed in a variety of natural membranes. The steady-state conductance increases exponentially, changing e-fold every 3-10 mV, and approaches a maximum at 150–200 mV (4, 6). Under voltage clamp the membrane currents in response to potential steps show a delayed rise and exponential decay and their time constants go through a maximum as a function of the potential (5, 7). Under certain conditions there also appears inactivation with properties very similar to that observed in muscle or nerve (5). As in nerve, muscle, and other excitable tissues, the conductance changes can be described quantitatively by inserting the proper parameters into the Hodgkin and Huxley (H & H) equations (8).

It is generally agreed that ions cross the membrane through localized, sparsely distributed channels and that the ion selectivity of the channels is controlled by their molecular structure (9). The different ion specificities seen in a variety of excitable cells and the diversity of the above compounds should not distract from the fact that the gating phenomena in these cells and in lipid bilayers are identical, and that the basic molecular mechanism by which the membrane opens and closes for the passage of ions could be essentially the same in all cases.

We propose here a detailed molecular model for the gating process, placing particular emphasis on alamethicin, because of the three compounds mentioned above it is the only one with known structure (10) (Fig. 1A). We believe, however, that the same ideas apply to monazomycin and EIM, and beyond that – with some modification – to the ion gating systems of higher cells. The model is an explicit molecular realization of the original H & H formulation, and is consistent with their suggestion that the potential controls the position of charged particles in the membrane, leading to the formation of a bridge or chain for the flow of ions.

THE MODEL

Figure 1A shows the structure of alamethicin. The ring symmetry is interrupted at two locations: a glutamic acid–glutamine residue (location 17 and 18) protruding into the ring at the top, and a glutamine side chain (location 6) visible at lower right. The molecule can be folded into the elongated shape of Fig. 1B. Here the glutamic acid–glutamine residues are seen at the top. One half of the ring is essentially in β-configuration, its carbonyl oxygens facing to one side. The other half is partly α-helix and hydrophobic. The hairpin bend at the lower end of the molecule together with the glutamine side chain form a cavity lined with carbonyl oxygens, containing a metal ion in four- or five-fold coordination. Because the glutamine side chain is not exactly opposite the two top residues, it is not only ideally suited to form part of the metal ion coordinating cavity, but can also stabilize by hydrogen bonding the sharp folding of the amino acid backbone at the bottom of the molecule opposite the two top residues. Once in this shape and after binding a metal ion, alamethicin has a large dipole moment, due to the carboxyl anion of the glutamine (location 18) at one end and the chelated cation at the other end. The molecule is approximately 36 Å long and, as shown in Fig. 1B, is large enough to span the hydrocarbon region of a bilayer.

Accepting for the moment this conformation of alamethicin, we can design a gating

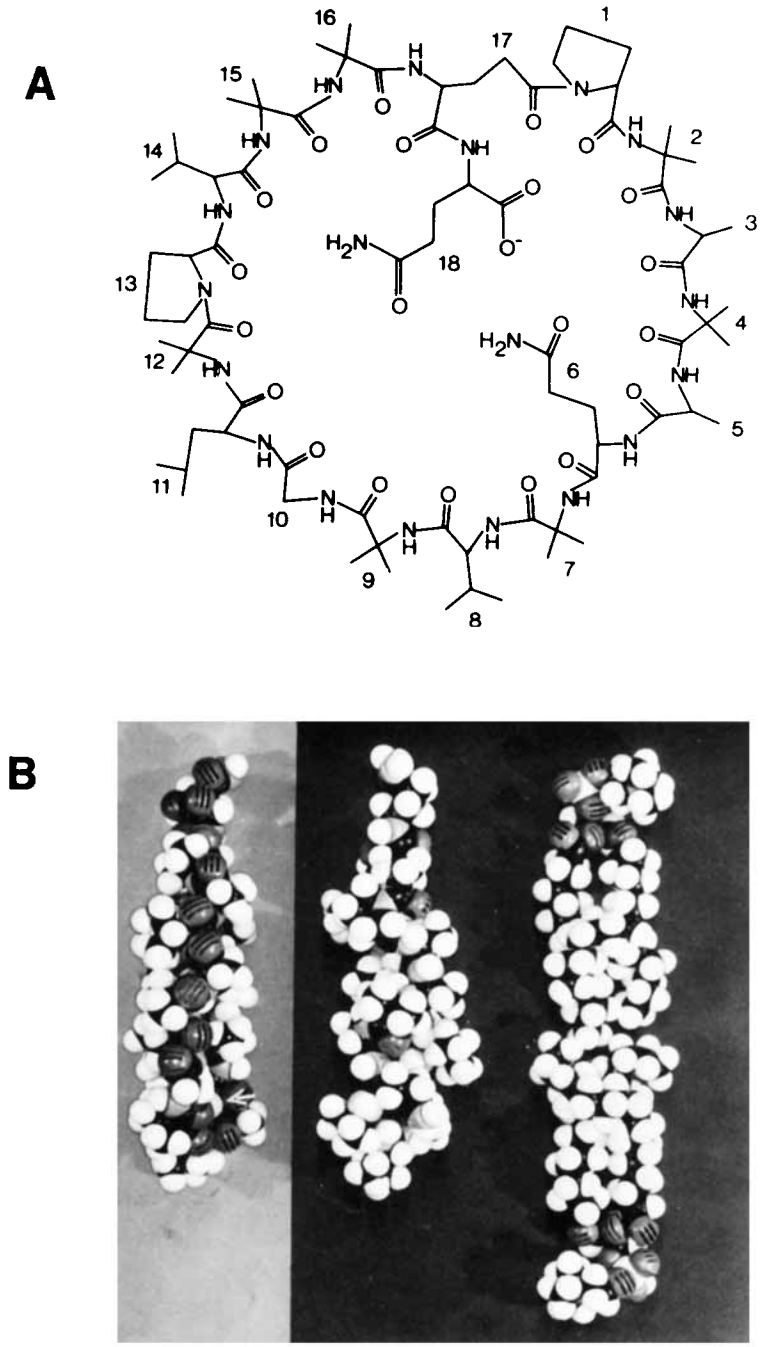

Fig. 1. (A) The structure of alamethicin [after Payne et al. (10)]. (B) Left and center: a proposed molecular configuration of alamethicin, viewed from 2 sides. The metal ion is visible at the lower end of the molecule at the left (arrow). Right: two lecithin molecules in bilayer configuration.

mechanism consistent with the molecular features and the experimental observations. We assume that at rest, i.e., in the absence of an applied field, the majority of the alamethicin molecules adsorbed from solution to the membrane lies flat on the (cis) membrane surface (Fig. 2A). An applied field of the proper direction (positive on the side of the alamethicin) tilts the molecules by pulling the metal ion containing end through the hydrocarbon region to the opposite (trans) membrane surface, so that they now span the membrane, their long axis normal to the membrane plane and parallel to the lipid hydrocarbon chains (Fig. 2B). The hydrophilic residues 17 and 18 keep one end of the molecule attached to the original surface.

Rapid lateral diffusion of the monomers within the membrane plane leads to their sequential aggregation into dimers, trimers, tetramers, etc. (Fig. 2C). In these aggregates the α-helix sides of the molecules face outward, their hydrocarbon side chains interacting with the lipid hydrocarbons, while the carbonyl oxygens on the other side face toward the center forming the wall of a hydrophilic channel (Fig. 3). The channel diameter is determined by the number of monomers per channel and their dimensions. Monomers and dimers do not form an open channel. The stability conditions for a particular n-mer may vary with the lipid, but it stands to reason that pentamers or hexamers are preferred. Ions move through the channel either hydrated or nonhydrated depending on the channel diameter. Upon removal of the applied field, the free monomers return to their original surface. The channels break up into monomers which also go to the surface, and the membrane returns to its high resistance state. The elongated shape of the alamethicin need not necessarily persist at the surface, but may only originate after insertion into the hydrocarbon phase.

SUPPORTING DATA AND ARGUMENTS

Aside from being consistent with the H & H formulation and its molecular interpretation, the model has a number of consequences agreeing well with the observations.

Low Resting Conductance

Because in the low conductance state the alamethicin is assumed to lie at the membrane surface, the membrane resistance in that state should be as high as that of the unperturbed bilayer, i.e., 10^7 to 10^8 Ω cm^2, an expectation borne out by experiment (5, 6). At higher alamethicin concentration some monomers can enter the membrane and form channels in the absence of an applied field, giving rise to a conductance at zero membrane potential.

Gating Charge

One chelated metal ion per alamethicin is needed as a "gating charge" to pull the molecule into the membrane. As a consequence the conductance should be (and has been measured to be) the same high power function of the metal ion concentration as that of alamethicin (4). If the metal ion is divalent, the applied field is twice as effective, and the conductance–voltage relation is twice as steep (6).

Gating Current

The movement of the metal ion across the bilayer would give rise to a gating

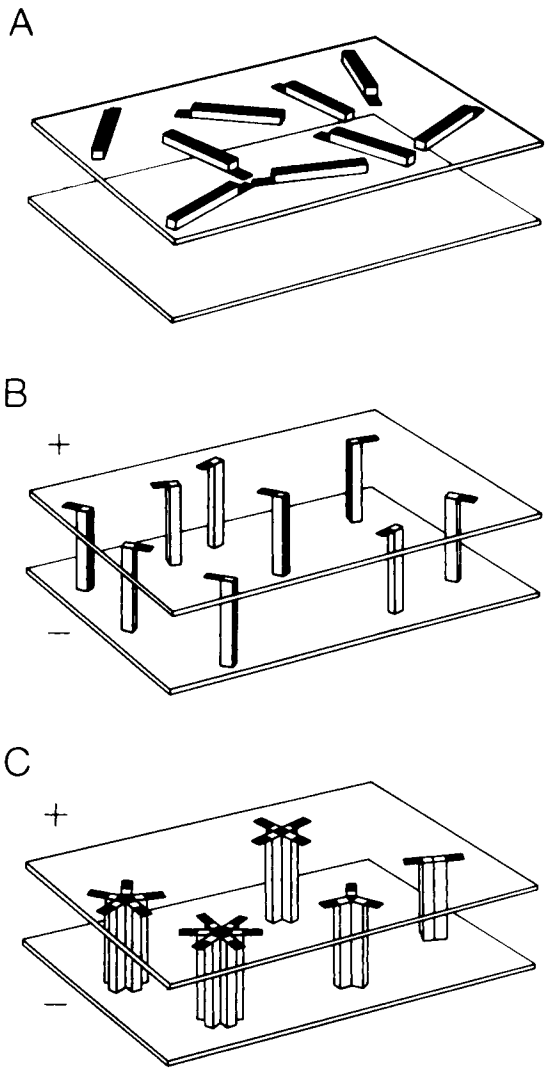

Fig. 2. A model of the excitation process. (A) At rest, abstract models of alamethicin molecules lie flat on the membrane surface represented by the upper plane. The extension at one end of the molecules represents the glutamic residues. (B) An applied field acting on the metal ion has pulled the molecules into the membrane toward the trans surface. (C) Lateral diffusion within the membrane leads to aggregation of the monomers into oligomers. Trimers, tetramers, pentamers, and hexamers form a central opening acting as a channel for the flow of ions.

current, and whereas for technical reasons gating currents have not yet been observed in artificial membranes, they have been demonstrated in the Na system of the squid axon (11). It should be noted in this connection that for energetic reasons, the conductance–voltage relation requires that the gating charge utilize most or all of the field energy, i.e., it must cross the entire hydrocarbon region as it does in this model (8).

Position of the Conductance–Voltage Curve

The position of the conductance–voltage curve with respect to the voltage axis, i.e., the potential region over which the gating occurs, depends on several parameters; one is the interaction of the channel former with the surface as determined by hydrogen bonding, dipole, and polar forces. Dipole and polar forces are susceptible to modification by the surface potential. Shifts of the conductance–voltage curve along the voltage axis by agents affecting the surface potential are well known in nerve (12, 13) and artificial membranes (3, 5, 14, 15) and are consistent with the model. Another parameter is the self-interaction of the monomers inside the hydrocarbon region. If it is high, the equilibrium is shifted toward the aggregates, i.e., channels, and at zero membrane potential the number of channels could be relatively high. This is the case with EIM (and perhaps nerve), where a resting potential of 60 mV is necessary to keep the conductance low. Finally, polar groups (in the case of alamethicin the chelated metal ion) pulled through the membrane may interact with lipid polar groups and water at the trans-membrane surface, anchor the molecule in that position, and stabilize the aggregated form.

Gate Polarization

It is apparent for two reasons that the gating mechanism is polarized across the membrane: first, potentials of only one sign increase the conductance and, second, upon removal of the field the system returns to the original state. If the channel formers are added to both membrane sides, two separate conducting systems result, each being opened and closed independently by fields of opposite sign (4, 14). The effect is a natural consequence of the model because as long as one end of the alamethicin stays firmly attached to the cis side of the membrane, the molecule will return to that side after removal of the field. If the channel former is relatively small, monomers may be pulled or may diffuse through the membrane resulting in gating action from both sides. In certain lipids this can happen to alamethicin and to monazomycin (5, 14). It is significant that methylation of the glutamic carboxyl group in alamethicin increases this effect (16), presumably by reducing the charge and interaction of this region with the membrane surface groups, allowing the entire molecule to diffuse across the membrane.

Concentration Effects

Because the channel is an oligomer the conductance measured at any potential should be a high order function of the alamethicin concentration at the membrane surface and, within limits, in the water phase. For the same reason the time constants of the conductance changes should decrease strongly with the monomer concentration. Both effects can be demonstrated with all three compounds.

Lipid Fluidity Effects

After the monomers have been inserted into the membrane, the rate of channel formation depends not only on their self-interaction parameters, but also on the lateral diffusion rates of monomers and channels. It is therefore of particular interest that the time constants of the conductance changes depend strongly on the fluidity of the lipid used to form the bilayer. For alamethicin the time constants in glycerol diolein (GDO) membranes are as low as 200 μsec, i.e., as short as those of the Na system of nerve (Fig. 4A). Judging from NMR data (17) these membranes have a much lower viscosity than

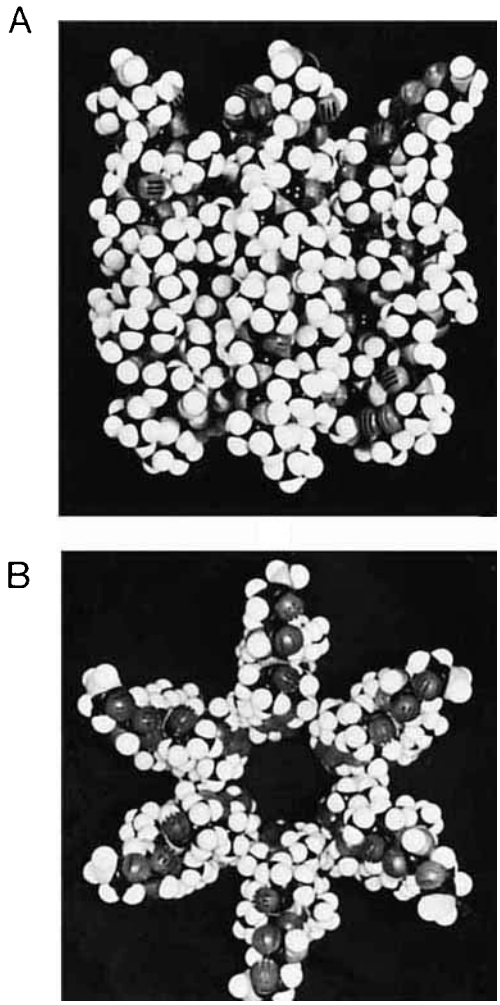

Fig. 3. A molecular model (CPK) of a hexameric channel formed by the aggregation of 6 alamethicin molecules. (A) Side view; (B) Top view.

phospholipid membranes. In oxidized cholesterol membranes, on the other hand, time constants of several seconds are usual (Fig. 4B). This change of the time constants takes place with only minor changes of the inherent kinetics, i.e., the system still follows the basic H & H description. Similar changes, although by only two orders of magnitude, can be demonstrated with monazomycin. The observed high temperature coefficients of the rate of conductance change may also partly reflect viscosity changes of the lipids.

Self-Interaction

The strong self-interaction of alamethicin required by the model is evident from its aggregation in aqueous solution (18) and from its insolubility in hydrocarbon solvents. Its surface viscosity at an air–water interface is one hundred times as great as that of a

typical lipid. Monazomycin is also insoluble in hydrocarbon solvents. EIM apparently has a higher molecular weight, and its very strong aggregation tendency, with aggregate weights exceeding 10^6 daltons (19), may be the reason why it is in the conducting state at zero membrane potential.

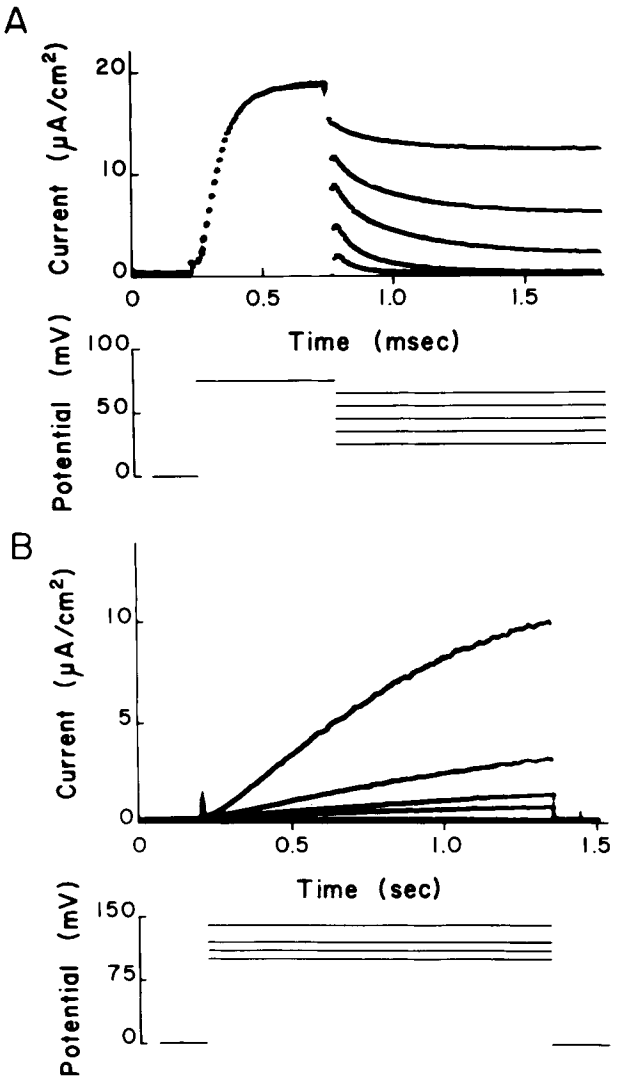

Fig. 4. Membrane currents (top) in response to potential steps (bottom) for two different membranes in the presence of alamethicin. The records in (A) were obtained from a membrane containing a high percentage of glycerol diolein (glycerol diolein/diolein phosphate/octane in volume ratios of 0.2:0.05:1). The membrane-forming solution in (B) contained 40 mg oxidized cholesterol and 50 mg dodecyl phosphate in 1 cc of octane. Several oscillograph sweeps were superimposed at 20 sec intervals. Although the time scales differ by a factor of 1000 in the two records, the general shape of the currents is preserved showing a delayed and sigmoid rise. (A) also demonstrates the exponential decay of the currents in response to a potential decrease and the variation of the time constants with the potential. The time constants are comparable to those in nerve.

Instantaneous Conductance–Voltage Relation

The instantaneous conductance of the channels agrees with the proposed channel structure. The current–voltage curves of an unmodified bilayer, as well as the instantaneous current–voltage relation of the open monazomycin and alamethicin channels, follow a sinh function. This is typical of a barrier diffusion mechanism (20). The mechanism is well understood for the unmodified membrane (21), in which the field pulls the ions crossing the membrane away from the surface multipole of the lipid polar groups into the hydrocarbon region. Because the alamethicin channels are large (as determined by single channel experiments) the ions must pass almost fully hydrated, and the barrier causing the sinh function may be due to the repulsive potential of the chelated metal ions (in the case of alamethicin) or the amino groups (in the case of monazomycin) forming a ring at the trans side of the channel. It should be pointed out that the instantaneous current–voltage curves in nerve are reported to be linear. However, the data available so far have been obtained only between ± 60 mV, a region where the bilayer current–voltage curves are also linear.

Single Channels

One of the strongest arguments for the proposed mechanism can be made on the basis of single channel measurements with alamethicin. Individual conductance steps were originally observed with EIM (3, 22, 23) and interpreted as single channel gating events. They have now been reported for alamethicin, gramicidin, and other systems (24–26). With alamethicin, in certain lipids, the conductance steps occur in bursts, the conductance varying rapidly between five or six clearly defined levels (Fig. 5A). The spacing of the levels is not uniform but increases in a characteristic manner, the intermediate levels being most frequently occupied. If the alamethicin channel were built up successively from monomers into dimers, trimers, etc., via interposition of monomers and conversely degraded, the bunching of conductance steps and increasing step size would be a direct and quantitative consequence. As a matter of fact, the values of the conductance levels reported by Gordon and Haydon (24) can be calculated directly from the molecular dimensions of the oligomeric channels (Fig. 5B). The conductance of a channel built from n alamethicin molecules if

$$g_n = \frac{\chi}{l} A \qquad (1)$$

with $A = 0.25\ ns^2 \cot(180°/n)$. A represents the area of regular polygons with side length, s, (= 7.9 Å) derived from the width of the alamethicin monomer. The specific conductance of the aqueous phase χ is equal to $0.11\ \Omega^{-1}\ cm^{-1}$, assuming a 5:1 K/Cl transference number ratio for the open channel and 2 M KCl which is the concentration used to obtain the data of Fig. 5A. The channel length, l, (= 25 Å) is obtained from the length of the hydrophobic region of the alamethicin molecule (Fig. 1B). The exact fit of the data may be fortuitous, but the fact that the conductance levels increase in the same manner as the area of regular polygons speaks strongly for a sequential increase of the channel diameter by the interposition of monomers.

The conductance steps usually start at the lowest level and disappear through that level (25), indicating that the alamethicin channels are built up and degraded by the sequential addition and removal of monomers. Pentamers and hexamers seem to be most

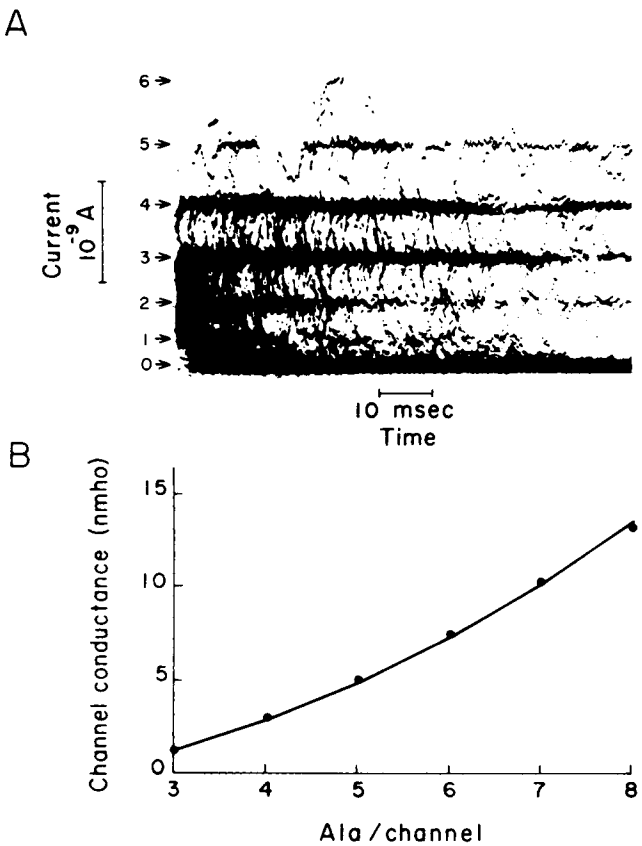

Fig. 5. (A) Current fluctuations through a lipid bilayer membrane (glycerol monoleate) in the presence of 10^{-8} mol/l alamethicin [after Gordon and Haydon (24)]. The membrane potential was clamped at 210 mV. The aqueous phase contained 2 M KCl. Many sweeps were superimposed on the screen of a storage oscilloscope, each sweep being triggered by the leading edge of a current transition. The baseline corresponds to the conductance of an unmodified bilayer. Six different current levels can be distinguished (arrows) and their relative probability of occurrence can be estimated from the intensity of the baseline traces. The 3rd and 4th levels are the most probable. The spacing between the levels increases with the current. (B) Correlation between the conductance levels calculated from (A) and the conductance of hypothetical channels formed by the aggregation of 3 to 8 alamethicin molecules. The points represent the conductance levels and are obtained from the current levels in (A). The lowest level (1) is assumed to correspond to the conductance of a trimer. The curve represents the conductance of single channels built from 3–8 alamethicin molecules as shown in Figs. 2 and 3. It was calculated from Eq. 1 for integral values of n. The curve segments for nonintegral values of n have no meaning within the framework of the model.

stable because the average lifetime of the different conductance levels centers strongly around the third and fourth level. Higher levels are very rare. This distribution of conductance occurs at the lowest observable alamethicin concentration, i.e., when there is only one channel. As the concentration of monomers inside the membrane is increased, either by the addition of more alamethicin or by the applied potential, the average life-

time of the individual n-mers must, for theoretical reasons, increase approximately as the nth power of the concentration. Thus, at high concentrations practically all channels are in the hexameric configuration, and the time spent in lower configurations is very short.

Not all lipids show this temporal grouping of gating events, and it is not a necessary consequence of the model. The relative stability of the different n-mers could be very much dependent on the lipid properties, so that in some cases only hexamers are stable and are built up very rapidly via lower n-mers. Alternatively, the folding of a linear chain of six monomers into a circle would give rise to only one conductance step. Finally, if the channels were built from single peptide chains the lower n-mers could have openings smaller than the ion diameter and only pentamers or hexamers may be conductive. It is therefore possible to build a defined, energetically favored channel structure by this mechanism without too much contribution to the conductance from the other less favored channel configurations. There is currently no direct evidence for these alternatives, but it should be noted that noise analysis of the Na channels in nerve suggests that they are not gated by a one-step open–close mechanism, but by a multistep process (27).

Quantitative Description of the Model

The proposed gating mechanism consists of two separate reactions: one is the insertion of the channel-forming molecules into the hydrocarbon region and their orientation normal to the membrane plane by the applied field, and the other is their subsequent lateral diffusion and aggregation into a channel. The process can be formally described by a scheme of the form

$$
\begin{aligned}
& P_0 \underset{k_{10}}{\overset{k_{01}}{\rightleftharpoons}} P_1 \\
P_1 + P_n & \underset{k_{(n+1)(n)}}{\overset{k_{(n)(n+1)}}{\rightleftharpoons}} P_{n+1} \qquad (2) \\
P_1 + P_{m-1} & \underset{k_{(m)(m-1)}}{\overset{k_{(m-1)(m)}}{\rightleftharpoons}} P_m
\end{aligned}
$$

where P_0 represents the concentration of monomers resting at the surface, P_1 that of inserted monomers, P_2 to P_n that of the dimers, trimers, etc., P_m being the largest n-mer. The total concentration of channel formers, C, is represented by

$$
C = P_0 + \sum_{n=1}^{m} nP_n \qquad (3)
$$

The rate constants controlling the insertion of monomers k_{01} and k_{10} are assumed to be voltage-dependent and of the form

$$k_{01,10} = Z \cdot \exp\left(-\frac{E_{01,10} \mp 0.5zV \cdot 23.05}{RT}\right) \quad (4)$$

Z is the frequency factor, E the activation energy for the insertion process, z the valency of the charge on which the membrane potential V acts and 23.05 the conversion factor from electron-volt to kcal/mole. The sign of the voltage is taken as positive on the side of the alamethicin. The rate constants k_{01} and k_{10} correspond to the α and β in the H & H formulation. The other rate constants are of the form:

$$k_{(n)\,(n+1)} = Z \cdot \exp\left(-\frac{E_{(n)\,(n+1)}}{RT}\right) \quad (5)$$

$$k_{(n+1)\,(n)} = Z \cdot \exp\left(-\frac{E_{(n+1)\,(n)}}{RT}\right) \quad (6)$$

In first approximation they are not voltage-dependent and determined by the interaction energies and diffusion rates of the various fractions. This assumption is justified by the observation that for alamethicin only the "off" times of the individual single channel conductance levels shorten with increased potentials, whereas the "on" times of each individual step are little or not at all affected indicating that the average time between the insertion of a monomer into an n-mer and its exit depends only on its inherent interaction energies, and not on the voltage.

The concentration P_n of the different n-mers as a function of time and voltage can be derived from Eqs. 2–6 by numerical methods from the corresponding differential rate equations and the total membrane conductance g in Ω^{-1} cm^{-1} from

$$g = \sum_{n=3}^{m} N_n \cdot g_n \quad (7)$$

where g_n is the conductance of the individual n-mer and the number of n-mers per cm^2 is

$$N_n = N \cdot \delta \cdot P_n \cdot 10^{-3} \quad (8)$$

N is Avogadro's number, δ the membrane thickness and P_n the n-mer concentration.

Kinetic Consequences of the Model

When the aggregation rates are much higher than the insertion rate, and only one oligomer configuration (e.g., the tetramer) is energetically preferred (but less preferred than the monomer), the above formulation reduces to the H & H equations. Under these conditions the time constants of the observed clamping currents are only dependent on the field and not on the state of the system. This leads to the superposition of currents

from different prepotentials as demonstrated by Cole and Moore (28). Such ideal behavior is observed with alamethicin or monazomycin in very liquid lipids (e.g., GDO) or at high temperature.

However, important and clear deviations from the ideal behavior appear in more viscous lipids, e.g., cholesterol–dodecyl phosphate mixtures. In these membranes the aggregation process can become rate-limiting such that several relaxation times appear under appropriate pulsing sequences. Figure 6A demonstrates a particularly instructive case for alamethicin. The calculated conductance derived from numerical solutions of the above reaction scheme is shown for comparison in Fig. 6B. EIM and monazomycin can display the same phenomenon. Many more details of the aggregation reaction can be demonstrated by voltage clamp techniques. They have been theoretically analyzed and all effects are found to agree with this theory.

Inactivation

The formation of channels by sequential aggregation leads directly and without additional assumptions to inactivation, provided that nonconducting channel precursors, e.g., dimers, are energetically preferred or that their formation is retarded. Calculations have shown that under these conditions the channel concentration goes through a maximum in time. Such an aggregation overshoot has been experimentally demonstrated for virus coat protein aggregation (33) and for a polynucleotide phosphorylase (34). The calculated gating kinetics match quantitatively the properties of the Na system in nerve, including the recently observed gating currents. One example is shown in Fig. 6D. The calculations also predict some experimental details such as the Hoyt shift not accounted for by the H & H equations (31, 32).

Voltage-Dependent Aggregation

The simple assumption, that the aggregation rate constants are independent of the membrane potential, may not always be justified. There are indications that for all three channel formers, the interaction energies of at least the early stages of aggregation are directly controlled by the potential. These effects may be explained by the somewhat graded and incomplete insertion of the channel former into the membrane, so that at low voltage only part of the molecules extend into the hydrocarbon region. In this case an approximate formulation giving a satisfactory fit to the data assumes aggregation rate constants of the form

$$k_{(n)\,(n+1)} = Z \cdot \exp\left(-\frac{E_{(n)\,(n+1)} - W_n \cdot f(V)}{RT}\right) \tag{10}$$

$$k_{(n+1)\,(n)} = Z \cdot \exp\left(-\frac{E_{(n+1)\,(n)} + W_n \cdot f(V)}{RT}\right) \tag{11}$$

$$f(V) = \frac{\exp\left(-\frac{\epsilon_1 - qV \cdot 23.05}{RT}\right)}{\exp -\left(\frac{\epsilon_1 - qV \cdot 23.05}{RT}\right) + \exp -\left(\frac{\epsilon_2 + qV \cdot 23.05}{RT}\right)} \tag{12}$$

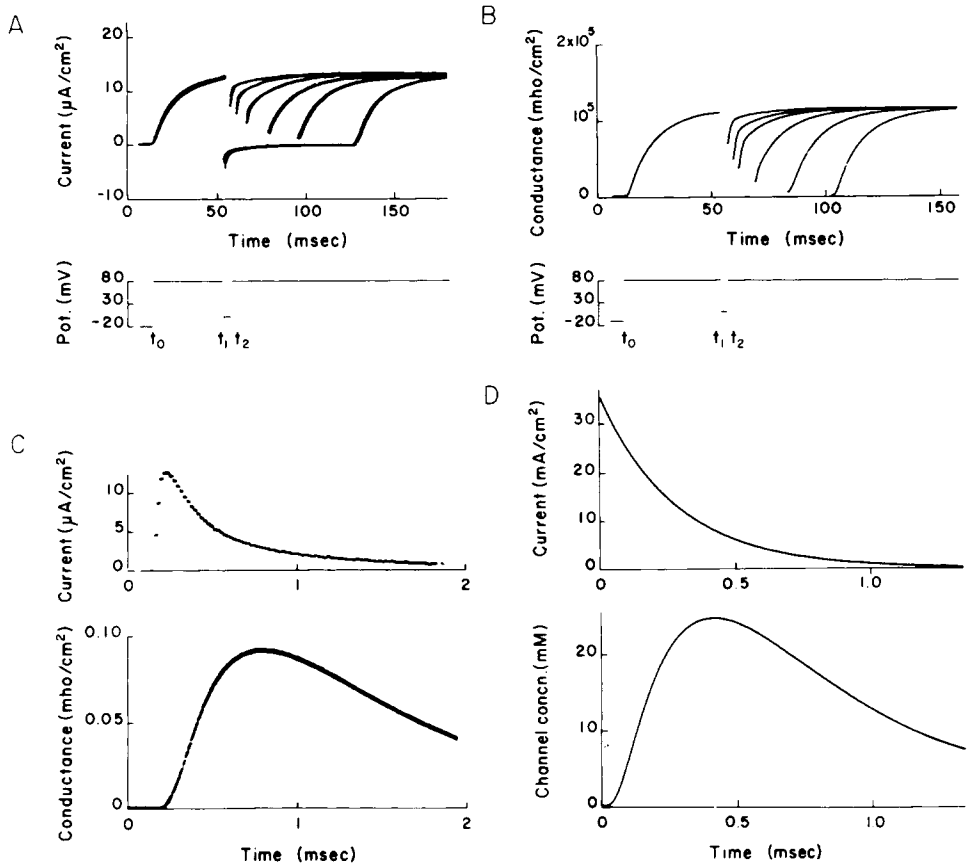

Fig. 6. (A) Membrane currents (upper record) in response to voltage steps (lower record) from a lipid bilayer in the presence of 10^{-6} M alamethicin. At t_0 a positive voltage of 80 mV causes a delayed current. At t_1 the membrane is clamped to −10 mV for a brief period, until t_2, when the potential is returned to +80 mV. After that (not visible in the record) the potential is returned to the holding value of −20 mV. The pulsing sequence is repeated every 10 sec increasing t_2 from 60 to 130 msec. Successive sweeps are superimposed. During the −10 mV pulse the membrane conductance falls exponentially, as is apparent from the instantaneous currents upon repolarization to +80 mV at t_2. At short t_2 the consequent current rise has two time constants, indicating that the time course of the conductance changes depends not only on the membrane potential as required by the H & H theory, but also on the state of the system. (B) Calculated conductance changes for the same pulse sequence as in (A). The curves were calculated from Eqs. 7 and 8, obtaining P_n by numerical solution of the differential rate equations for the reaction scheme Eq. 2, with rate constants according to Eqs. 4–6, assuming that the largest n-mer is a hexamer. For clarity, the conductance decay during the +10 mV pulse is not drawn. The following constants were used: $C = 1$, $Z = 10^4$, $z = 2$, $E_{01} = 3$, $E_{10} = 1$, $E_{12} = 2.5$, $E_{21} = 1$, $E_{23} = 2$, $E_{32} = 2.5$, $E_{34} = 1$, $E_{43} = 2$, $E_{45} = 0.5$, $E_{54} = 1$, $E_{56} = 0.5$, $E_{65} = 0$. In the model, the state dependence of the time constants results mainly from the retention of nonconducting channel precursors, i.e., monomers and dimers, in the hydrocarbon region during the +10 mV pulse.

(C) The relation between the gating current (upper record) and conductance (lower record) in the squid axon Na system. The records represent the response of the axon to a depolarizing potential step [after Armstrong (11)]. (D) The same relation as calculated from the model. The calculations were done as in (B) except that only the hexamer was assumed to be conductive. Therefore the lower curve represents the number of hexameric channels as a function of time. The upper curve shows the current due to the entry of monomers into the membrane. It was obtained by multiplying $-dP_0/dt$ by the Faraday constant. The potential step was from −80 to 60 mV. The following constants were used: $C = 1$, $Z = 3 \times 10^6$, $z = 2$, $E_{01} = 5.4$, $E_{10} = 6.6$, $E_{12} = 3$, $E_{21} = 7$, $E_{23} = 1.5$, $E_{32} = 1.5$, $E_{34} = 1$, $E_{43} = 2.5$, $E_{45} = 0.5$, $E_{54} = 0.5$, $E_{56} = 0$, $E_{65} = 1.7$. The number of channels and therefore the conductance goes through a maximum as a function of time, i.e.; the system shows inactivation. This occurs because nonconducting dimers are energetically preferred and their formation is slow relative to the formation of higher n-mers, which form rapidly and later decay again into dimers.

f (V) modifies the interaction energies between the monomers and the different n-mers as a function of the potential. The constants ϵ and q control the range over which the potential is effective. The general form of f (V) is such that it varies between 0 and 1 and saturates at low and high voltages. This form was chosen because we assumed that the interaction energies depend on the insertion depth of the n-mer into the membrane. With this additional assumption the model can account quantitatively for a set of complex kinetic features observable under appropriate conditions with all three compounds. particularly with monazomycin. The example of Fig. 7 gives some indication of these effects and illustrates that such complexities could follow directly from the proposed aggregation mechanism.

Absolute Reaction Rates

It should be noted that for the sake of computational simplicity the calculations assumed a total concentration of channel formers, C, of 1 M. For this reason the values of g in Fig. 6B appear extremely high. In reality $10^{-4}-10^{-6}$ M is the average measured value of C for alamethicin in the lipid phase (29). For such concentrations the free energies of the monomer–n-mer interaction required to fit the kinetic data are 5 to 8 kcal/mol, values which make the numerical integration extremely cumbersome. Nevertheless, even at these low concentrations, theoretical estimates of the absolute reaction rate are in fair agreement with the observed values. In a viscous medium the collision frequency, Z, is

$$Z = 8 \pi \sigma ND \cdot 10^{-3} \qquad (9)$$

where σ is the molecular diameter, N Avogadro's number, and D the diffusion coefficient (30). Values of 10^{-8} cm^2 sec^{-1} for D, and 20 Å for a σ give encounter frequencies of 3×10^7 l sec^{-1} mol^{-1}. Allowing for an increase by a factor of 100 (due to the solvent cage effect) and neglecting steric effects, the calculated overall time constants of the conductance changes are between 10 and 100 msec, i.e., within the range found for phospholipids. In order to account for the much smaller time constants in GDO lipids, the diffusion coefficient must be either as high as 10^{-6} cm^2 sec^{-1}, or aggregation of the surface monomers (perhaps via hydrogen bonding) leads to locally restricted spots of high surface concentration and consequently to higher reaction rates. The latter possibility may be true for the Na and K systems of nerve.

Other Gating Systems

The general nature of the gating mechanism is also supported by what is known so far about monazomycin: it has the typical molecular weight, composition, IR, and fluorescence spectra of the cyclic polyene antibiotics containing a sugar presumably at one end of the elongated molecule, and an amino group which – if located opposite the sugar – could act as gating charge in place of the chelated metal ion in alamethicin. If monazomycin were a polyene, the channels would contain only one row of hydrophilic groups per molecule instead of two as in alamethicin. Consequently, the channel diameter should increase by smaller amounts, perhaps explaining the absence of observable single channel events. Several polyenes, e.g., amphotericin and nystatin, are known to form channels which are not, however, voltage-dependent. Their structure lacks the bipolarity

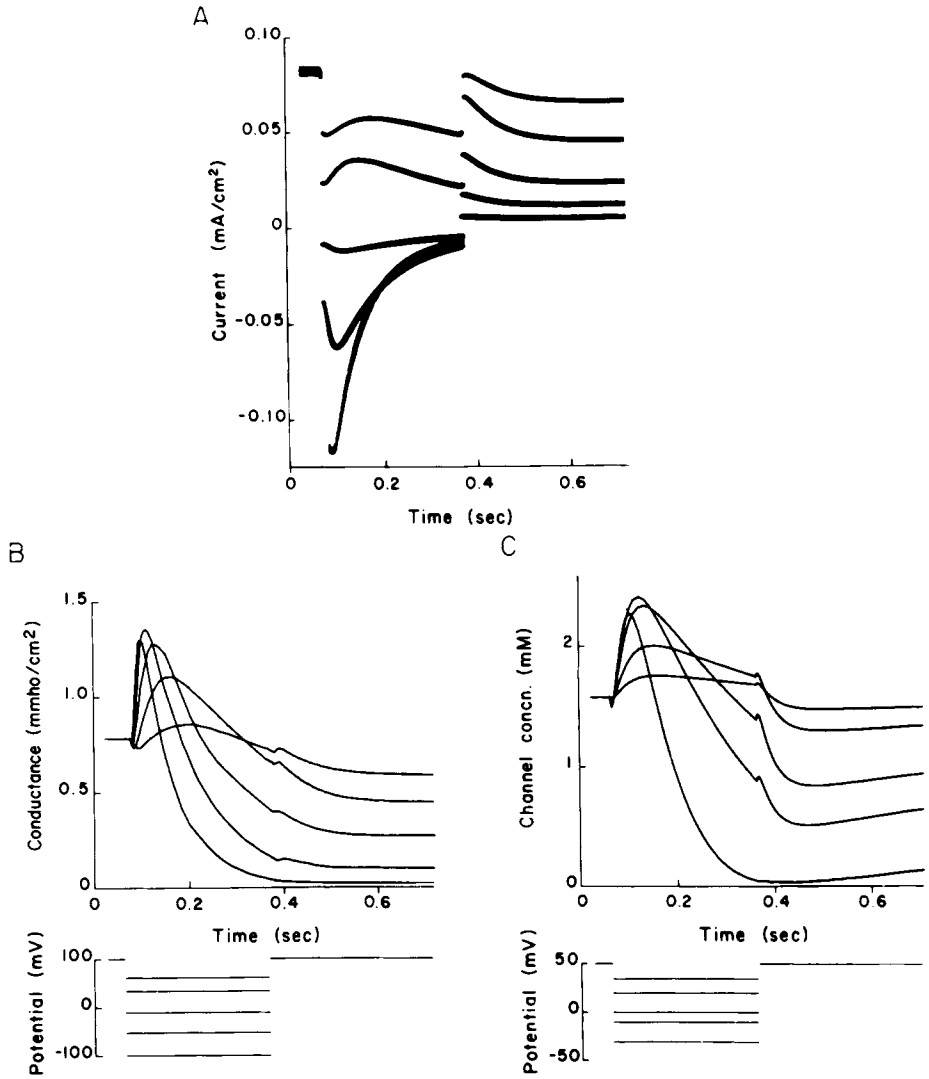

Fig. 7. (A) Membrane currents in response to potential steps (shown in B) from a bilayer in 0.01 M NaCl in the presence of 10^{-6} M monazomycin on one side. The membrane solution contained 100 mg oleylphosphate and 50 mg cholesterol in 1 cc of octane. Five sweeps were superimposed on a storage scope. The potential steps were applied at 10 sec intervals. The current transients start from 0.08 mA cm^{-2} corresponding to the high conductance at the holding potential of 100 mV (positive on the side of monazomycin). Their sign inverts as the potential of the step becomes negative. Because of the slow sweep speed, the usual capacitance transients lasting only 100 μsec are not visible. (B) The membrane conductance changes derived from the currents in (A). Note the initial decrease followed by a rise and subsequent exponential fall. At the end of the potential step the sign of these transients inverts and their time course is slower. The transients disappear at temperatures above 40°C and are absent in less viscous lipids (GDO). Under such conditions the conductance decays exponentially during a negative potential, i.e., shows only the ideal H & H time course. (C) Channel concentration as a function of time and voltage as calculated from the model assuming that the aggregation rate constants are voltage-dependent. Equations 4 and 10–12 were used for the rate constants, and as in Fig. 6D, it was assumed that only the hexamer is conductive. The following constants were used: C = 1, Z = 100, z = 2, E_{01} = 4, E_{10} = 2, E_{12} to E_{65} = 0, ϵ_1 = 2, ϵ_2 = 2, q = 0.5, W_1 = 2, W_2 = 0.5, W_3 = 0.5, W_4 = 0.4, W_5 = 0.4. In the model the transient conductance increase, in response to potentials which lower the steady-state conductance, has the following origin: As a result of voltage-dependent dimer breakdown the concentration of monomers inside the membrane increases temporarily causing a transient build-up of conducting hexamers from lower n-mers. The effect is dependent on a fast decay of dimers and a slower removal of inserted monomers to the surface.

necessary for the gating action. Instead, the molecules may be permanently anchored across the membrane (35), their long axis spanning the hydrocarbon region, but forming essentially the same oligomeric channel structure as suggested for alamethicin.

As yet little is known about the structure of EIM. The monomer seems to be larger than alamethicin and may contain several peptide side arms which could be pulled through the membrane under the influence of the field, aggregating with others from neighboring EIMs to form a channel. Trypsin blocks the conductance from the trans side, liberating arginine and suggesting that the arginine amino group plays the role of the gating charge. EIM does not seem to permeate the membrane in totality, i.e., the gating action remains polarized, and because of that and its stronger tendency to be "open" at zero voltage it may be structurally somewhat closer to the channel formers in nerve.

A search among the polyenes of known structure showed that $DJ400B_2$ (36) fulfills the minimal conditions for voltage-dependent gating required by the model: i) it is bipolar, containing an amino sugar and a carboxyl group at one end and an amino group at the other, ii) it is long enough to span the hydrocarbon region, iii) it has polar groups along one side to form the hydrophilic channel interior and hydrophobic regions (the polyene chain) to interact with the lipid hydrocarbons, and iv) it aggregates in hydrophobic solvents. As expected, $DJ400B_2$ induces voltage-dependent gating similar to alamethicin.

DISCUSSION

The model is based on the insertion of channel formers into the lipid bilayer and their subsequent aggregation to form a channel.

The aggregation depends on the lateral diffusion of the oriented channel precursors in a fluid lipid phase. The liquidity of the bilayer region in cell membranes is well established (37–39). Rotational and translational diffusion of membrane proteins in the membrane plane have been demonstrated (40, 41), and the antibody-triggered aggregation of membrane-bound antigens (42) bears a strong resemblance to the proposed aggregation of channel precursors. The orientation of membrane proteins across the membrane by hydrophilic groups interacting with one or both membrane interfaces has also been postulated (43).

There are many possible conformations for the alamethicin. In our porposed structure the peptide bonds have been kept in trans-planar conformation. The rotational angles, Φ and Ψ, have been kept within the constraints given by steric overlap and near-neighbor contact energy considerations. This conformation does not agree with the lowest energy form calculated by Burgess and Leach (44). It can be argued, however, that the hydrophobic and polar interactions of the lipid hydrocarbons and the channel water are sufficiently anisotropic to cause a considerable deviation from the preferred conformation in free space. In fact a large part of the stabilization energy of the channel may result from the interaction between the peptide carbonyls and water molecules inside the channel. The assumption that one side of the ring contains a helical segment is consistent with optical data (18), but need not be true. Both sides could be in a straight chain conformation with their carbonyl groups facing mainly to one side, the hydrocarbon side chains to the other. This would increase the channel side width of the alamethicin monomer to 9.5 Å, but also increase the channel length. Since both effects compensate, single channel conductance measurements do not allow one to distinguish between the two alternatives.

Some details of the proposed mechanism remain unclear. For instance, it is neither known if the trimer or the tetramer is the lowest conducting configuration, nor if monomers or dimers are pulled into the membrane by the field. Furthermore, the molecules may aggregate at the surface prior to insertion, thus increasing the local concentration and with it the rate constants. Such secondary modifications would not alter the kinetic phenomena as long as the sequential aggregation mechanism is preserved.

In contrast to most excitable cells none of the gated channels in the bilayer shows a significant selectivity for different cations. The reason for this discrepancy is not clear. It may be either that the nature or spacing of the hydrophilic groups inside the channel is different, or that the ionic selectivity rests in a separate structure located at the channel entrance, acting as a sieve for a specific ion. Examples of the latter possibility are seen with EIM and alamethicin where the adsorption of basic proteins from the aqueous phase can invert the channel selectivity from cationic to anionic without changing the gating properties. Another example may be the appearance of potassium selectivity in channels formed by perimycin after succinilation of its amino group.

In the proposed configuration, the channel constituting part of the alamethicin molecule is slightly shorter than the lipid hydrocarbon region, so that in an applied field the end of the molecule containing the gating charge does not reach the opposite polar region of the bilayer. This fact assures that the gating action is rapidly reversible, because if the gating charge could reach the other side, its interaction with the polar interface or the water would hold the molecule in a position spanning the bilayer and prevent the channels from closing.

The model could also apply to more complex molecular structures. For example, one or more peptide side arms attached to a globular protein body may, after insertion into the membrane by the field, aggregate with side arms of neighboring units to form oligomeric channels.

We suggest that the model also applies to the excitation process of higher cells. This suggestion rests primarily on the analogies between bilayers and cells with respect to steady-state and kinetic phenomena. Alternate excitation models (45, 46) based on allosteric mechanisms are conceivable, but are still rather arbitrary. In nerve, deviations from the ideal H & H kinetics have been reported (32) and state-dependent rate constants have been described (47), but a systematic search for effects like those in Figs. 6 and 7 is still lacking. Such effects, if seen, could further strengthen, but not settle, the argument for a common mechanism, and as long as the molecular structures involved are unknown, the issue must remain open.

The model may also account for the action of local and general anesthetics in cell membranes and excitable bilayers. In the context of the model local anesthetics would alter the charge or dipole characteristics of the membrane surface, shifting the conductance voltage curves, whereas the general anesthetics may enter the hydrocarbon regions and prevent the aggregation of the channel-forming monomers.

The electrical field need not be the only driving force for the insertion and aggregation of channel precursors. In cells there may be structures where instead the binding of ligands serves this purpose, leading to receptor function and, perhaps in more complex structures, to ion transport.

ACKNOWLEDGMENTS

Alamethicin was kindly supplied by G. B. Whitfield, Jr., monazomycin by E. L. Patterson, and DJ400B_2 by E. V. Dehmlow. We appreciate the technical assistance of Ana L. Young, Patricia Lewis, Mike Ewald, Charles Williams, Sandra Montimore, Hadassah Freifelder, and Young Chew Chock, and thank D. O. Rudin for stimulating discussions and comments. This research was partially supported by a grant from the National Science Foundation (BMS68-0073).

REFERENCES

1. Meyer, C. E., and Reusser, F., Experientia 23:85 (1967).
2. Mitscher, L. A., Shay, A. J., and Bohonos, N., Appl. Microbiol. 15:1002 (1967).
3. Mueller, P., and Rudin, D. O., J. Theor. Biol. 18:222 (1968).
4. Mueller, P., and Rudin, D. O., Nature 217:713 (1968).
5. Mueller, P., and Rudin, D. O., In "Current Topics in Bioenergetics," (R. D. Sanadi, Ed.), 3:157. Academic Press, New York (1969).
6. Cherry, R. J., Chapman, D., and Graham, D. E., J. Membrane Biol. 7:325 (1972).
7. Muller, R. U., and Finkelstein, A., J. Gen. Physiol. 60:263 (1972).
8. Hodgkin, A. L., and Huxley, A. F., J. Physiol. 117:500 (1952).
9. Hille, B., In "Progress in Biophysics," (J. A. V. Butler and D. Noble, Eds.), 21:3. Pergamon Press, Oxford (1970).
10. Payne, J. W., Jakes, R., and Hartley, B. S., Biochem. J. 117:757 (1970).
11. Armstrong, C. M., and Bezanilla, F., Nature 242:459 (1973).
12. Chandler, W. K., Hodgkin, A. L., and Meves, H., J. Physiol., (London) 180:821 (1965).
13. Gilbert, D. L., In "Biophysics and Physiology of Excitable Membranes," (W. J. Adelman, Ed.), p. 359. Van Nostrand Reinhold, New York (1971).
14. Muller, R. U., and Finkelstein, A., J. Gen. Physiol. 60:285 (1972).
15. McLaughlin, S. G. A., Szabo, G., Eisenman, G., and Ciani, S. M., Proc. Nat. Acad. Sci. U.S. 67:1268 (1970).
16. Hall, J. E., personal communication.
17. Glaser, M., Simpkins, H., Singer, S. J., Sheetz, M., and Chan, S. I., Proc. Nat. Acad. Sci. U.S. 65:721 (1970).
18. McMullen, A. I., and Stirrup, J. A., Biochim. Biophys. Acta 241:807 (1971).
19. Bukovsky, J., personal communication.
20. Frenkel, J., "Kinetic Theory of Liquids," Vol. 40. Dover Publications, Inc., New York (1955).
21. Kauffman, J. W., and Mead, C. A., Biophys. J. 10:1084 (1970).
22. Ehrenstein, G., Lecar, H., and Nossal, R., J. Gen. Physiol., 55:119 (1970).
23. Bean, R. C., Shepherd, W. C., Chan, H., and Eichner, J., J. Gen. Physiol. 53:741 (1969).
24. Gordon, L. G. M., and Haydon, D. A., Biochim. Biophys. Acta 255:1014 (1972).
25. Eisenberg, M., Hall, J. E., and Mead, C. A., J. Membrane Biol. 14:143 (1973).
26. Hladky, S. B., and Haydon, D. A., Nature 225:451 (1970).
27. Fishman, H. M., Proc. Nat. Acad. Sci. U.S. 70:876 (1973).
28. Cole, K. S., and Moore, J. W., Biophys. J. 1:1 (1960).
29. Chelack, W. S., and Petkau, A., J. Lipid Res., 14:255 (1973).
30. Smoluchowski, M. V., Zeits, Phys. Chem. 92:129 (1917).
31. Hoyt, R. C., Biophys. J. 11:110 (1971).
32. Goldman, L., and Schauf, C. L., J. Gen. Physiol. 59:659 (1972).
33. Scheele, R. B., Schuster, T. M., and Khairallah, L. H., Abstracts 18th Annual Meeting Biophysical Society, 290a (1973).
34. Cantor, C. R., Biopolymers 6:369 (1968).

35. Finkelstein, A., and Holz, R., In "Membranes," (G. Eisenman, Ed.), 2:377 Marcel Dekker, Inc., New York (1972).
36. Bohlmann, F., Dehmlow, E. V., Neuhahn, H. J., Brandt, R., and Bethke, H., Tetrahedron 26:2199 (1970).
37. Hubbell, W. L., and McConnell, H. M., Proc. Nat. Acad. Sci. U.S. 61:12 (1968).
38. Steim, J. M., Tourtellotte, M. E., Reinert, J. C., McElhaney, R. N., and Rader, R. L., Proc. Nat. Acad. Sci. U.S. 63:104 (1969).
39. Singer, S. J., and Nicolson, G. L., Science 175:720 (1972).
40. Blasie, J. K., Worthington, C. R., and Dewey, M. M., J. Molec. Biol. 39:407 (1969).
41. Matus, A., de Petris, S., and Raff, M. C., Nature New Biol. 244:278 (1973).
42. Frye, L. D., and Edidin, M., J. Cell Sci. 7:319 (1970).
43. Bretscher, M. S., Science 181:622 (1973).
44. Burgess, A. W., and Leach, S. J., Biopolymers 12:2691 (1973).
45. Changeux, J. P., Thiéry, J., Tung, Y., and Kittel, C., Proc. Nat. Acad. Sci. U.S. 57:335 (1967).
46. Hill, T. L., and Chen, Y. D., Biophys. J. 12:960 (1972).
47. Frankenhaeuser, B., and Hodgkin, A. L., J. Physiol. 137:218 (1957).